

L. F. Qian · R. C. Batra

Three-Dimensional transient heat conduction in a functionally graded thick plate with a higher-order plate theory and a meshless local Petrov-Galerkin method

Received: 16 December 2003 / Accepted: 22 July 2004 / Published online: 22 September 2004
© Springer-Verlag 2004

Abstract We analyze transient heat conduction in a thick functionally graded plate by using a higher-order plate theory and a meshless local Petrov-Galerkin (MLPG) method. The temperature field is expanded in the thickness direction by using Legendre polynomials as basis functions. For temperature prescribed on one or both major surfaces of the plate, modified Lagrange polynomials are used as basis and additional terms are added to these expansions to exactly match the given temperatures. Partial differential equations for the evolution of the coefficients of the Legendre polynomials are reduced to a set of coupled ordinary differential equations (ODEs) in time by a MLPG method. The ODEs are integrated by the central-difference method. The time history of evolution of the temperature at the plate centroid and through-the-thickness distribution of the temperature computed with the fifth-order plate theory are found to agree very well with those obtained analytically.

Keywords MLPG method · Effective thermal conductivity · Higher order plate theory · Inhomogeneous plate

1 Introduction

Advantages of functionally graded materials (FGMs) over laminated composites include the smooth variation of material properties in the body thereby eliminating the delamination mode of failure. For use in a severe thermal environment, FGM plates are designed so that

material properties vary continuously through the thickness from that of a ceramic on the side exposed to high temperature to that of a metal on the other side. For infinitesimal deformations of an initially unstressed elastic body, the balance of linear momentum and the heat equation governing the temperature distribution are one-way coupled in the sense that the heat equation can be solved first and then the computed temperature field can be used to find the mechanical displacements. One way to solve the heat equation analytically is to take the Laplace transform of the transient heat equation, solve the transformed equation by the series expansion method, and then take the inverse Laplace transform, e.g., see Vel and Batra [32]. These authors expanded the Laplace transformed temperature field and the material properties as a power series in the thickness coordinate, obtained a recursive relation for the unknowns which are solved for from the initial and boundary conditions. They then took the inverse Laplace transform. Sutrathar et al. [31] assumed that the thermal conductivity and the specific heat have the same exponential variation in one spatial direction, used Green's function for the heat equation, took the Laplace transform with respect to time of the simplified heat equation, solved the problem by the boundary element method, and finally took the inverse Laplace transform numerically to compute the temperature field. Jin and Batra [14] assumed that heat flows only in the direction in which material properties vary, the thermal conductivity varies exponentially and the thermal diffusivity is a constant. The one-dimensional heat equation then has an analytical solution. Kim and Noda [15] assumed that a FG plate with material properties varying in the thickness direction only can be considered as being made of several homogeneous laminae. The transient heat equation is solved in each lamina by using Green's function approach. The continuity conditions at the interfaces and boundary conditions at the top and the bottom surfaces are used to find the time dependent temperature field in the plate. Ootao and Tanigawa [22] also approximated a FG plate by a laminated one with each

L. F. Qian
Nanjing University of Science and Technology, Nanjing 210094,
P. R. China

R. C. Batra
Department of Engineering Science and Mechanics, M/C 0219
Virginia Polytechnic Institute and State University, Blacksburg,
VA 24061, USA
E-mail: rbatra@vt.edu

lamina made of a homogeneous material. Heat conduction in each layer was studied by taking the Laplace transform with respect to time and a double cosine series expansion in the two in-plane coordinates. Sutradhar et al. [31] cite other references that have used the Laplace transform and a numerical method to find an approximate solution of the transient heat equation. Sladek et al. [29] have used the meshless local boundary integral equation method to analyze transient heat conduction in a FG material.

In the thermomechanical analysis of linear elastic FG plates, the thermal problem is usually solved first either analytically or the temperature field is assumed to be known. The mechanical problem is then solved either numerically, analytically or by using a plate theory; e.g., see [22, 25, 26, 33, 34, 35] and references cited therein. Coupled nonlinear plane strain thermomechanical problems for FG bodies have been studied by Batra and Love [5]. Batra [4] analyzed plane strain static finite deformations of a FG cylinder made of a Mooney-Rivlin material.

Here we use a higher-order plate theory to determine transient thermal fields in a FG plate with material properties varying only in the thickness direction thereby setting the thermal problem on the same footing as the mechanical problem. The effective thermal conductivity is derived from that of the constituents of the FG plate by using a relation due to Hatta and Taya [13]. We note that Babuska, Lee and Schwab [3] have derived a posteriori estimates of modeling error for heat-

conduction in a plate. Rössle et al. [28] have employed the energy projection method to deduce a hierarchy of models for a linear elastic plate, and have also presented error estimates for the solution of the plate problem relative to that of the 3-D problem. These authors have also provided a historical background of the development of plate theories.

We use either orthonormalized Legendre polynomials or modified Legendre polynomials as basis functions to expand the temperature field in the thickness direction; the time-dependent coefficients of these Legendre polynomials are also functions of coordinates of a point on the midsurface of the plate. The series expansion for the temperature exactly satisfies the temperature boundary conditions prescribed on the top and/or the bottom surfaces of the plate. Partial differential equations for determining the coefficients of Legendre polynomials are derived by the principle of “virtual work”. The two-dimensional initial-boundary-value problem is reduced to a system of coupled ordinary differential equations in time by a meshless local Petrov-Galerkin method (MLPG) proposed by Atluri and Zhu [1]. Alternatively, one could have used a finite element (FE) method or another meshless method such as the element-free Galerkin [9], the hp-clouds [11], the reproducing kernel particle [18], the smoothed particle hydrodynamics [19], the modified smoothed particle hydrodynamics (MSPH) [38] the diffuse element [21], the partition of unity finite element [20], the natural element [30], and meshless

Table 1 Comparison of the MLPG and the FE methods for a transient problem

	MLPG	FEM
Weak form	Local	Global
Information needed about nodes	Locations only	Locations and connectivity
Subdomains	Circular/rectangular, not necessarily disjoint	Polygonal and disjoint
Basis functions	Complex and difficult to express in closed form	Simple polynomials
Integration rule	Higher order	Lower order
Satisfaction of essential boundary conditions	Requires extra effort	Easy to enforce
Mass/stiffness matrices	Asymmetric, large band width that can not be determined <i>a priori</i> , not necessarily positive semidefinite	Symmetric, banded, mass matrix positive definite, stiffness matrix positive definite after imposition of essential boundary conditions.
Sum of elements of mass matrix	Not necessarily equal to the total mass of the body	Equals total mass of the body
Assembly of equations	Not required	Required
Stresses/strains/heat flux	Smooth everywhere	Good at integration points
Locking phenomenon for constrained problems	No	Yes
Addition of nodes	Easy	Difficult
Determination of time step size for stability in an explicit algorithm	Difficult, requires determination of the maximum frequency of the structure	Relatively easy
Computation of the total strain energy of the body	Difficult	Relatively easy
Imposition of continuity conditions at interfaces between two materials	Requires either consideration in the generation of basis functions or the use of Lagrange multipliers	Easy to implement
Data preparation effort	Little	Extensive
CPU time	Considerable	Relatively little

Galerkin method using radial basis functions [37]. Meshless methods have become popular because nodes can be placed at arbitrary locations. The finite-difference method and the collocation technique are also meshless methods of finding an approximate solution of a given boundary-value problem. These methods and other developments on meshless methods are discussed in two recent books [2, 17]. For transient heat conduction in a bimetallic circular disk, Batra et al. [6] have used two MLPG formulations coupled with either the method of Lagrange multipliers or the method of jump function to account for the discontinuity in the temperature gradient at the interface between two different materials. Warlock et al. [36] used the method of Lagrange multipliers to enforce traction conditions at a rough contact surface during the analysis of static deformations of a linear elastic material enclosed in a rectangular cavity.

Advantages of the MLPG method are that it employs a local weak formulation of the problem and no background mesh is required to numerically evaluate various integrals appearing in the local Petrov-Galerkin formulation of the problem. However, a higher-order integration rule is generally needed to evaluate these integrals. The Table 1 compares the MLPG and the FE methods.

As far as we can ascertain, this is the first attempt to use a plate theory for studying transient heat conduction in a FG thick plate.

For a thick FG plate, the temperature field computed with the first six Legendre polynomials as basis functions (i.e., a 5th-order plate theory) is found to agree very well with the analytical solution of the problem.

2 Formulation of the problem

2.1 Governing equations and weak formulation

A schematic sketch of the problem studied and the rectangular Cartesian coordinate axes used to describe

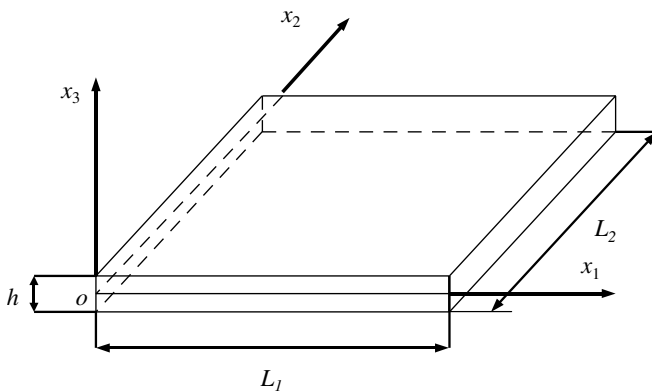


Fig. 1 Schematic sketch of the problem studied

heat conduction in the FG plate are shown in Fig. 1. S denotes the midsurface of the plate and Γ its boundary. It is assumed that the macroscopic response of the plate can be modeled as isotropic and its material properties vary smoothly in the thickness direction only.

The heat conduction in the absence of an internal heat source is governed by

$$\begin{aligned} \rho c \dot{\theta} &= -q_{i,i}, \text{ in } \Omega \times (0, T), \\ q_i &= -\kappa \theta_{,i} \text{ in } \Omega \times (0, T), \\ q_i n_i &= \bar{q} \text{ on } (\partial_q \Omega = S_q^+ \cup S_q^- \cup (\Gamma_q \\ &\quad \times [-h/2, h/2])) \times (0, T), \\ \theta &= \bar{\theta} \text{ on } (\partial_\theta \Omega = S_\theta^+ \cup S_\theta^- \cup (\Gamma_\theta \\ &\quad \times [-h/2, h/2])) \times (0, T), \\ \theta(x_1, x_2, x_3, 0) &= \theta_0(x_1, x_2, x_3) \text{ in } \Omega. \end{aligned} \quad (1)$$

Here ρ , c and κ are, respectively, the mass density, the specific heat and the thermal conductivity of a material point, $\Omega = S \times [-h/2, h/2]$ is the region occupied by the body, and S_q^+ (S_θ^+) and S_q^- (S_θ^-) are parts of the top and the bottom surfaces where the heat flux (the temperature) is prescribed respectively. Γ_q and Γ_θ are parts of the boundary ∂S of S where the heat flux and the temperature are prescribed as \bar{q} and $\bar{\theta}$ respectively. The initial temperature distribution in the body is given by $\theta_0(x_1, x_2, x_3)$. A comma followed by i indicates partial differentiation with respect to x_i , and a superimposed dot indicates partial differentiation with respect to time t . A repeated index implies summation over the range of the index, and \mathbf{n} is a unit outward normal to the surface. Equation (1)₁ expresses the balance of internal energy for a rigid body, Eq. (1)₂ is the Fourier law of heat conduction, Eqs. (1)₃ and (1)₄ are boundary conditions, and Eq. (1)₅ is the initial condition that is assumed to be consistent with the prescribed boundary conditions.

Let η be a smooth function defined on Ω . Multiplying both sides of Eq. (1)₁ with η , integrating the resulting equation over Ω , using the divergence theorem for the term on the right-hand side of the equation and boundary conditions (1)₃ and (1)₄, we get

$$\int_{\Omega} \rho c \eta \dot{\theta} d\Omega + \int_{\Omega} \kappa \theta_{,i} \eta_{,i} d\Omega + \int_{\partial_q \Omega} \bar{q} \eta dA - \int_{\partial_\theta \Omega} \kappa \theta_{,i} n_i \eta dA = 0. \quad (2)$$

In the Galerkin FE formulation of the problem, one usually requires that $\eta = 0$ on $\partial_\theta \Omega$. However, in the MLPG formulation, it is not necessary to require that $\eta = 0$ on $\partial_\theta \Omega$ since essential boundary conditions are satisfied either by the penalty method or by the method of Lagrange multipliers or by suitably modifying the stiffness matrix, the mass matrix and the load vector. Equation (2) is a weak formulation of the problem.

2.2 Higher-order plate theory

For simplicity, we assume that either the heat flux or the temperature is prescribed on all of S^+ and/or S^- . Also, we do not derive 2-dimensional field equations and the associated boundary conditions for the temperature. The approach followed here is similar to that used by Batra and Vidoli [7] and Batra et al. [8] who derived a higher-order shear and normal deformable plate theory (HOSNDPT) for piezoelectric and elastic plates respectively. They used a mixed variational principle and postulated constitutive relations for fluxes. Here we derive heat flux from the assumed temperature field and the Fourier law of heat conduction; such a theory is called compatible HOSNDPT in [8].

2.2.1 Heat flux prescribed on the top and the bottom surfaces of the plate

Let $L_\alpha(x_3)$, $\alpha = 0, 1, 2, \dots, K$ be Legendre polynomials defined on $[-h/2, h/2]$ and orthonormalized according to the relation

$$\int_{-h/2}^{h/2} L_\alpha(z)L_\beta(z)dz = \delta_{\alpha\beta}, \quad (3)$$

where $\delta_{\alpha\beta}$ is the Kronecker delta. Expressions for L_0, L_1, \dots, L_5 are given below.

$$\begin{aligned} L_0(x_3) &= \frac{1}{\sqrt{h}}, & L_1(x_3) &= 2\sqrt{\frac{3}{h}}\frac{x_3}{h}, \\ L_2(x_3) &= \frac{1}{2}\sqrt{\frac{5}{h}}\left[12\left(\frac{x_3}{h}\right)^2 - 1\right], \\ L_3(x_3) &= \sqrt{\frac{7}{h}}\left[-3\left(\frac{x_3}{h}\right) + 20\left(\frac{x_3}{h}\right)^3\right], \\ L_4(x_3) &= \frac{3}{\sqrt{h}}\left[\frac{3}{8} - 15\left(\frac{x_3}{h}\right)^2 + 70\left(\frac{x_3}{h}\right)^4\right], \\ L_5(x_3) &= \sqrt{\frac{11}{h}}\left[\frac{15}{4}\left(\frac{x_3}{h}\right) - 70\left(\frac{x_3}{h}\right)^3 + 252\left(\frac{x_3}{h}\right)^5\right]. \end{aligned} \quad (4)$$

The temperature $\theta(x_1, x_2, x_3, t)$ at any point in the plate is approximated by

$$\theta(x_1, x_2, x_3, t) = \sum_{\alpha=0}^K L_\alpha(x_3)\tilde{\theta}_\alpha(x_1, x_2, t), \quad (5)$$

where $\tilde{\theta}_\alpha(x_1, x_2, t)$ is the temperature at time t at the point (x_1, x_2) of the midsurface S of the plate. Thus

$$\begin{Bmatrix} \partial\theta/\partial x_1 \\ \partial\theta/\partial x_2 \\ \partial\theta/\partial x_3 \end{Bmatrix} = \sum_{\alpha=0}^K L_\alpha(x_3) \begin{Bmatrix} \partial\tilde{\theta}_\alpha/\partial x_1 \\ \partial\tilde{\theta}_\alpha/\partial x_2 \\ \sum_{\beta=0}^K d_{\beta\alpha}\tilde{\theta}_\beta \end{Bmatrix} \equiv \sum_{\alpha=0}^K \{\lambda_\alpha\}\tilde{\theta}_\alpha, \quad (6)$$

where

$$\{\lambda_\alpha\} = \begin{Bmatrix} L_\alpha(x_3)\frac{\partial}{\partial x_1} \\ L_\alpha(x_3)\frac{\partial}{\partial x_2} \\ \sum_{\beta=0}^K d_{\alpha\beta}L_\beta(x_3) \end{Bmatrix}, \quad (7)$$

$$d_{\alpha\beta} = \int_{-h/2}^{h/2} \frac{dL_\alpha}{dx_3}(x_3)L_\beta(x_3)dx_3. \quad (8)$$

Analogous to Eq. (5), we write

$$\eta(x_1, x_2, x_3) = \sum_{\alpha=0}^K L_\alpha(x_3)\tilde{\eta}_\alpha(x_1, x_2). \quad (9)$$

Substituting from eqs. (5), (6) and (9) into (2) and carrying out the integration with respect to x_3 from $-h/2$ to $h/2$, we get

$$\begin{aligned} & \int_S \tilde{\eta}_\alpha M_{\alpha\beta} \dot{\tilde{\theta}}_\beta dA + \int_S \tilde{\eta}_\alpha k_{\alpha\beta} \tilde{\theta}_\beta dA \\ & + L_\alpha\left(\frac{h}{2}\right) \int_{S^+} \bar{q}\tilde{\eta}_\alpha dA + L_\alpha\left(-\frac{h}{2}\right) \int_{S^-} \bar{q}\tilde{\eta}_\alpha dA \\ & + \int_{\Gamma_q} \tilde{\eta}_\alpha \ell_\alpha ds - \int_{\Gamma_\theta} \tilde{\eta}_\beta p_{\beta\alpha} \tilde{\theta}_\alpha ds = 0, \end{aligned} \quad (10)$$

where

$$\begin{aligned} M_{\alpha\beta} &= \int_{-h/2}^{h/2} \rho c L_\alpha L_\beta dx_3, \\ k_{\alpha\beta} &= \int_{-h/2}^{h/2} \kappa \{\lambda_\alpha\} \{\lambda_\beta\}^T dx_3, \\ \ell_\alpha &= \int_{-h/2}^{h/2} \bar{q}(s, x_3) L_\alpha(x_3) dx_3, \\ p_{\alpha\beta} &= \int_{-h/2}^{h/2} \kappa \{n\}^T \{\lambda_\alpha\} L_\beta(x_3) dx_3. \end{aligned} \quad (11)$$

Here s is the arc length along the boundary ∂S of S . In Eq. (10) quantities are defined on the midsurface S of the plate, and elements of $k_{\alpha\beta}$ and $p_{\alpha\beta}$ involve differential operators with respect to in-plane coordinates.

2.2.2 Temperature prescribed on the top and the bottom surfaces of the plate

For plates made of an elastic material, surface tractions are most often prescribed on the top and the bottom surfaces of a plate. However, in a thermal problem, it is often assumed that the temperature is assigned on one or both of the major surfaces of the plate. One way to incorporate the prescribed temperature field into the problem formulation is to use the method of Lagrange multipliers and hypothesize an

augmented functional. An alternative is to consider trial solutions that identically satisfy the temperature boundary conditions on the major surfaces of the plate. The first approach introduces two Lagrange multiplier functions that need to be determined as a part of the solution of the problem. This is analogous to finding pressure field in incompressible materials. The second approach does not introduce additional unknowns and is adopted here. Stipulating trial solutions that also identically satisfy prescribed temperatures at the plate edges limits the class of functions in the space of trial solutions. Hence, essential or Dirichlet boundary conditions at the plate edges are satisfied either by the method of Lagrange multipliers, or the penalty method or by suitably modifying the heat capacity and the conductivity matrices and the load vector.

Let $\tilde{L}_\alpha(x_3)$, $\alpha = 0, 1, 2, \dots, K$ be modified Legendre polynomials of degree $K + 2$ that satisfy the conditions

$$\int_{-h/2}^{h/2} \tilde{L}_\alpha(x_3) L_\beta(x_3) dx_3 = \delta_{\alpha\beta}, \quad \alpha, \beta = 0, 1, 2, \dots, K,$$

$$\tilde{L}_\alpha(h/2) = 0, \quad \tilde{L}_\alpha(-h/2) = 0. \quad (12)$$

That is, \tilde{L}_α is orthogonal to the $(K + 1)$ Legendre polynomials L_0, L_1, \dots, L_K , and vanishes at $x_3 = \pm h/2$. For $K = 3$, solutions of Eqs. (12) are

$$\begin{aligned} \tilde{L}_0(x_3) &= \frac{\sqrt{2}}{16} \left(5 + 120 \left(\frac{x_3}{h} \right)^2 - 560 \left(\frac{x_3}{h} \right)^4 \right), \\ \tilde{L}_1(x_3) &= \frac{1}{16} \sqrt{\frac{2}{3}} \left(-42 \frac{x_3}{h} + 1680 \left(\frac{x_3}{h} \right)^3 - 6048 \left(\frac{x_3}{h} \right)^5 \right), \\ \tilde{L}_2(x_3) &= \frac{1}{10} \sqrt{\frac{2}{5}} \left(-35 + 840 \left(\frac{x_3}{h} \right)^2 - 2800 \left(\frac{x_3}{h} \right)^4 \right), \\ \tilde{L}_3(x_3) &= \frac{1}{16} \sqrt{\frac{2}{7}} \left(-374 \left(\frac{x_3}{h} \right) + 5040 \left(\frac{x_3}{h} \right)^3 - 14176 \left(\frac{x_3}{h} \right)^5 \right). \end{aligned} \quad (13)$$

The temperature distribution in the plate is assumed to be given by

$$\begin{aligned} \theta(x_1, x_2, x_3, t) &= \sum_{\alpha=0}^K \tilde{L}_\alpha(x_3) \tilde{\theta}_\alpha(x_1, x_2, t) \\ &+ \frac{1}{2} [\theta^+(x_1, x_2, t) + \theta^-(x_1, x_2, t)] \\ &+ \frac{x_3}{h} [\theta^+(x_1, x_2, t) - \theta^-(x_1, x_2, t)]. \end{aligned} \quad (14)$$

Note that (14) satisfies the prescribed temperature boundary conditions on the top and the bottom surfaces of the plate. Recalling (6), we obtain from (14)

$$\begin{Bmatrix} \partial\theta/\partial x_1 \\ \partial\theta/\partial x_2 \\ \partial\theta/\partial x_3 \end{Bmatrix} = \sum_{\alpha=0}^K \{ \tilde{\lambda}_\alpha \} \tilde{\theta}_\alpha + [\mu] \begin{Bmatrix} \theta^+ \\ \theta^- \end{Bmatrix}, \quad (15)$$

where

$$[\mu] = \begin{bmatrix} \left(\frac{1}{2} + \frac{x_3}{h} \right) \frac{\partial}{\partial x_1} & \left(\frac{1}{2} - \frac{x_3}{h} \right) \frac{\partial}{\partial x_1} \\ \left(\frac{1}{2} + \frac{x_3}{h} \right) \frac{\partial}{\partial x_2} & \left(\frac{1}{2} - \frac{x_3}{h} \right) \frac{\partial}{\partial x_2} \\ \frac{1}{h} & -\frac{1}{h} \end{bmatrix}, \quad (16)$$

and $\{ \tilde{\lambda}_\alpha \}$ is given by (7) with $L_\alpha(x_3)$ replaced by $\tilde{L}_\alpha(x_3)$.

Substituting for θ from (14) and for η from (9) into (2), carrying out the integration with respect to x_3 from $-h/2$ to $h/2$, we obtain the following equation for the determination of $\tilde{\theta}_\alpha$.

$$\begin{aligned} \int_S \tilde{\eta}_\alpha \tilde{M}_{\alpha\beta} \tilde{\theta}_\beta dA + \int_S \tilde{\eta}_\alpha \tilde{N}_\alpha dA + \int_S \tilde{\eta}_\alpha \tilde{k}_{\alpha\beta} \tilde{\theta}_\beta dA + \int_S \tilde{\eta}_\alpha \tilde{P}_\alpha dA \\ + \int_{\Gamma_q} \tilde{\eta}_\alpha \tilde{\ell}_\alpha ds - \int_{\Gamma_0} \tilde{\eta}_\alpha \tilde{p}_{\alpha\beta} \tilde{\theta}_\beta ds + \int_{\Gamma_0} \tilde{\eta}_\alpha R_\alpha ds = 0, \end{aligned} \quad (17)$$

where

$$\begin{aligned} \tilde{N}_\alpha &= \left(\int_{-h/2}^{h/2} \frac{\rho c}{2} \tilde{L}_\alpha dx_3 \right) (\theta^+ + \theta^-), \\ \tilde{P}_\alpha &= \left(\int_{-h/2}^{h/2} \kappa \{ \tilde{\lambda}_\alpha \} [\mu] dx_3 \right) \begin{Bmatrix} \theta^+ \\ \theta^- \end{Bmatrix}, \\ R_\alpha &= \left(\int_{-h/2}^{h/2} \kappa [n]^T [\mu] dx_3 \right) \begin{Bmatrix} \theta^+ \\ \theta^- \end{Bmatrix}, \end{aligned} \quad (18)$$

$\tilde{M}_{\alpha\beta}$, $\tilde{k}_{\alpha\beta}$, $\tilde{\ell}_\alpha$ and $\tilde{p}_{\alpha\beta}$ are given by (11) with $L_\alpha(x_3)$ replaced by $\tilde{L}_\alpha(x_3)$. Note that \tilde{N}_α , \tilde{P}_α and R_α depend upon the temperature prescribed on the top and the bottom surfaces of the plate.

2.2.3 Heat flux prescribed on the top and the temperature prescribed on the bottom surface of the plate.

In this case we require that the modified Legendre polynomials satisfy Eqs. (12)₁ and (12)₂ but not (12)₃. The temperature variation within the plate is given by (14) with $\theta^-(x_1, x_2, t)$ omitted. The rest of the analysis is similar to that of Sect. 2.2.2.

3 Meshless local Petrov-Galerkin formulation of the problem

Let M nodes be suitably placed on S , and S_1, S_2, \dots, S_M be smooth two dimensional closed regions, not necessarily disjoint and of the same shape and size, enclosing nodes $1, 2, \dots, M$ respectively. Let $\phi_1, \phi_2, \dots, \phi_N$ and $\psi_1, \psi_2, \dots, \psi_N$ with $N \leq M$ be two sets of linearly independent functions defined on one of these regions, say S_I , $1 \leq I \leq M$. We approximate $\tilde{\theta}(x_1, x_2, t)$ and $\tilde{\eta}(x_1, x_2)$ by

$$\begin{aligned}\tilde{\theta}_\alpha(x_1, x_2, t) &= \sum_{J=1}^N \phi_J(x_1, x_2) \delta_{J\alpha}(t) = \{\phi\}^T \{\delta_\alpha\}, \\ \alpha &= 0, 1, 2, \dots, K, \\ \tilde{\eta}_\alpha(x_1, x_2) &= \sum_{J=1}^N \psi_J(x_1, x_2) \hat{\delta}_{J\alpha} = \{\psi\}^T \{\hat{\delta}_\alpha\}, \\ \alpha &= 0, 1, 2, \dots, K,\end{aligned}\quad (19)$$

where $\delta_{J0}, \delta_{J1}, \dots, \delta_{JK}, J = 1, 2, \dots, N$ are fictitious values of nodal temperatures, and $\hat{\delta}_{J0}, \hat{\delta}_{J1}, \dots, \hat{\delta}_{JK}, J = 1, 2, \dots, N$ are arbitrary constants. We first derive below the semidiscrete formulation (or the ‘coupled ordinary differential equations for the ‘nodal’ temperatures $\delta_{J\alpha}$) for the case of the heat flux prescribed on the top and/or the bottom surfaces of the plate.

Replacing the domain S of integration in (10) by S_I , and substituting for $\tilde{\theta}$ and $\tilde{\eta}$ from (19), recalling that the resulting equation must hold for all choices of $\tilde{\eta}_\alpha$ and hence $\{\hat{\delta}_\alpha\}$, we obtain the following set of coupled ordinary differential equations (ODEs) for the determination of $\{\delta_\alpha\}$.

$$\begin{aligned}\sum_{J=1}^N H_{IJ} \dot{\delta}_{J\alpha} + \sum_{J=1}^N K_{IJ}^q \delta_{J\alpha} + F_{I\alpha}^q &= 0, \\ I &= 1, 2, \dots, N; \quad \alpha = 0, 1, 2, \dots, K,\end{aligned}\quad (20)$$

where

$$\begin{aligned}H_{IJ} &= \int_{S_I} \{\psi_I\} [M] \{\phi_J\}^T dA, \\ K_{IJ}^q &= \int_{S_I} \{\psi_I\} [k] \{\phi_J\}^T dA - \int_{\Gamma_\theta} \{\psi_I\} [p] \{\phi_J\}^T ds, \\ F_{I\alpha}^q &= L_\alpha \left(\frac{h}{2}\right) \int_{S^+} \bar{q} \{\psi_I\} dA \\ &\quad + L_\alpha \left(-\frac{h}{2}\right) \int_{S^-} \bar{q} \{\psi_I\} dA + \int_{\Gamma_q} \{\psi_I\} \ell_\alpha ds.\end{aligned}\quad (21)$$

Equation (20) is obtained for each S_I . There is no assembly of equations required in the MLPG method. Note that for each value of α in the range $0, 1, \dots, K$, a set of coupled ODEs needs to be integrated with respect to time t . Equations (20) and (21) are valid when the heat flux is prescribed on the top and the bottom surfaces of the plate.

For the case of the temperature prescribed on the top and the bottom surfaces of the plate, we substitute from (19) into (17) to arrive at the following set of coupled ordinary differential equations:

$$\begin{aligned}\sum_{J=1}^N H_{IJ} \dot{\delta}_{J\alpha} + \sum_{J=1}^N K_{IJ}^0 \delta_{J\alpha} + F_{I\alpha}^0 &= 0, \\ I &= 1, 2, \dots, N; \quad \alpha = 0, 1, 2, \dots, K,\end{aligned}\quad (22)$$

where

$$\begin{aligned}K_{IJ}^0 &= \int_{S_I} \{\psi_I\} [k] \{\phi_J\}^T dA + \int_{\Gamma_\theta} \{\psi_I\} [p] \{\phi_J\}^T ds, \\ F_{I\alpha}^0 &= \int_{S_I} \{\psi_I\} N_\alpha dA + \int_{S_I} \{\psi_I\} P_\alpha dA \\ &\quad + \int_{\Gamma_q} \{\psi_I\} \ell_\alpha ds + \int_{\Gamma_\theta} \{\psi_I\} R_\alpha ds.\end{aligned}\quad (23)$$

The basis functions $\{\phi_I\}$ are found by the moving least squares (MLS) method of Lancaster and Salkauskas [16]; it is described below briefly.

3.1 Brief description of the MLS basis functions

Let $f(x_1, x_2, t)$ be a scalar valued function defined on S_I ; f can be identified with the temperature field $\theta_\alpha(x_1, x_2, t)$. The approximation $f^h(x_1, x_2, t)$ is assumed to be given by

$$f^h(x_1, x_2, t) = \sum_{J=1}^m p_J(x_1, x_2) a_J(x_1, x_2, t), \quad (24)$$

where

$$\mathbf{p}^T(x_1, x_2) = \{1, x_1, x_2, (x_1)^2, x_1 x_2, (x_2)^2, \dots\}, \quad (25)$$

is a complete monomial in x_1 and x_2 having m terms. For example, $\mathbf{p}^T = \{1, x_1, x_2\}$ with $m = 3$ and $\mathbf{p}^T = \{1, x_1, x_2, (x_1)^2, x_1 x_2, (x_2)^2\}$ with $m = 6$ are, respectively, complete monomials of degree 1 and 2. The coefficients $a_1(x_1, x_2), a_2(x_1, x_2), \dots, a_m(x_1, x_2)$ are found by minimizing R defined by

$$R(\mathbf{x}) = \sum_{I=1}^n W(\mathbf{x} - \mathbf{x}_I) [\mathbf{p}^T(\mathbf{x}_I) \mathbf{a}(\mathbf{x}, t) - \hat{f}_I(t)]^2, \quad (26)$$

where $\hat{f}_I(t)$ is the fictitious value of $f^h(\mathbf{x}, t)$ at $\mathbf{x} = \mathbf{x}_I$, \mathbf{x}_I gives the location of node I , and n is the number of nodes ($m \leq n \leq N$) whose weight functions $W(\mathbf{x} - \mathbf{x}_I)$ have positive values at the point \mathbf{x} . Thus the weight function $W(\mathbf{x} - \mathbf{x}_I)$ is taken to be associated with the node I located at \mathbf{x}_I . Here we take

$$W(\mathbf{x} - \mathbf{x}_I) = \begin{cases} 1 - 6 \left(\frac{d_I}{r_w}\right)^2 + 8 \left(\frac{d_I}{r_w}\right)^3 - 3 \left(\frac{d_I}{r_w}\right)^4, & 0 \leq d_I \leq r_w, \\ 0, & d_I > r_w, \end{cases} \quad (27)$$

where $d_I = |\mathbf{x} - \mathbf{x}_I|$ is the distance between points \mathbf{x} and \mathbf{x}_I and r_w is the radius of the circle outside which W vanishes. r_w is called the support of the weight function W .

Setting $\partial R / \partial a_I = 0, I = 1, 2, \dots, m$ gives the following system of m linear algebraic equations for the determination of $a_1(\mathbf{x}), a_2(\mathbf{x}), \dots, a_m(\mathbf{x})$:

$$\mathbf{A}(\mathbf{x}) \mathbf{a}(\mathbf{x}, t) = \mathbf{P}(\mathbf{x}) \hat{\mathbf{f}}(t), \quad (28)$$

where

$$\begin{aligned} \mathbf{A}(\mathbf{x}) &= \sum_{I=1}^n W(\mathbf{x} - \mathbf{x}_I) \mathbf{p}^T(\mathbf{x}_I) \mathbf{p}(\mathbf{x}_I), \\ \mathbf{P}(\mathbf{x}) &= [W(\mathbf{x} - \mathbf{x}_1) \mathbf{p}(\mathbf{x}_1), \\ &\quad W(\mathbf{x} - \mathbf{x}_2) \mathbf{p}(\mathbf{x}_2), \dots, W(\mathbf{x} - \mathbf{x}_n) \mathbf{p}(\mathbf{x}_n)], \end{aligned} \quad (29)$$

are $m \times m$ and $m \times n$ matrices. Note that elements of these matrices depend upon the choice of the weight functions. Solving Eq. (28) for \mathbf{a} and substituting the result into (24) give

$$f^h(x_1, x_2, t) = \sum_{J=1}^n \phi_J(x_1, x_2) \hat{f}_J(t), \quad (30)$$

where

$$\phi_K(\mathbf{x}) = \sum_{J=1}^m p_J(\mathbf{x}) [\mathbf{A}^{-1}(\mathbf{x}) \mathbf{P}(\mathbf{x})]_{JK}, \quad K = 1, 2, \dots, n, \quad (31)$$

are the basis functions of the MLS approximation. Note that $\phi_J(\mathbf{x}_K) \neq \delta_{JK}$; thus $\hat{f}_J(t) \neq f^h(\mathbf{x}_J, t)$. For the matrix \mathbf{A} to be invertible, $n \geq m$. Equation (30) gives the value of $f^h(\mathbf{x}, t)$ in terms of the fictitious values $\hat{f}_J(t)$ of $f^h(\mathbf{x}, t)$ at n nodes whose weight functions are positive at the point \mathbf{x} . The value of n will vary with \mathbf{x} and the radius, r_w , of the compact support of $W(\mathbf{x} - \mathbf{x}_I)$. Here we take

$$r_w = bh_I, \quad (32)$$

where $h_I = \min\{|\mathbf{x}_J - \mathbf{x}_I|, 1 \leq J \leq N\}$ is the distance from the node at \mathbf{x}_I to the node nearest to it and b is a scaling parameter.

3.2. Basis functions for the test function

The choice $\psi_I(\mathbf{x}) = \phi_I(\mathbf{x})$ in Eq. (19)₂ will give a Galerkin formulation of the problem. However, it requires considerable computational resources to numerically evaluate integrals appearing in (21) or (23). Here we take $\psi_I(\mathbf{x}) = W(\mathbf{x} - \mathbf{x}_I)$ with $r_w = h_I$. Taking S_I also equal to a circle of radius h_I centered at the node at \mathbf{x}_I simplifies the evaluation of integrals appearing in Eq. (21) and (23) and preserves the local character of the MLPG formulation. For S_I completely inside S , boundary or line integrals in Eq. (21) and (23) identically vanish. When S_I intersects the boundary ∂S of S , then integrals in equations (21) and (23) are evaluated on $\partial S_I \cap \partial S$ and the line integrals need not vanish.

3.3. Evaluation of integrals

For S_I a circle of radius h_I , the area integrals in (21) and (23) are to be evaluated on a circular domain, and the line integrals on a part of the boundary of a circle. The circular region is mapped onto a $[-1, 1] \times [-1, 1]$ square region, and $N_g \times N_g$ Gauss integration points with the corresponding weights are used to numerically evaluate the integrals. In order to evaluate line integrals, the

circular arc is mapped onto $[-1, 1]$ and N_g Gauss points with the appropriate weights are used to evaluate the integrals.

3.4. Time integration of coupled ODEs

Equations (20) or (22) are integrated with respect to time t by the Crank-Nicolson method. That is, $\delta_{J\alpha}^t \simeq \delta_{J\alpha}(t)$ is evaluated from

$$\delta_{J\alpha}^{t+\Delta t} = \delta_{J\alpha}^t + \frac{\Delta t}{2} [\dot{\delta}_{J\alpha}^t + \dot{\delta}_{J\alpha}^{t+\Delta t}]. \quad (33)$$

Equation (20) is written at time $t + \Delta t$, and the value of $\dot{\delta}_{J\alpha}^{t+\Delta t}$ from (33) in terms of $\delta_{J\alpha}^{t+\Delta t}$, $\delta_{J\alpha}^t$ and $\dot{\delta}_{J\alpha}$ is substituted in it. The result is the following algebraic equation for $\delta_{J\alpha}^{t+\Delta t}$.

$$\begin{aligned} \frac{2}{\Delta t} \sum_{J=1}^N H_{IJ} \delta_{J\alpha}^{t+\Delta t} + \sum_{J=1}^N K_{IJ} \delta_{J\alpha}^{t+\Delta t} &= -F_{I\alpha}^q(t + \Delta t) \\ - \frac{2}{\Delta t} \sum_{J=1}^N H_{IJ} \delta_{J\alpha}^t - \sum_{J=1}^N H_{IJ} \dot{\delta}_{J\alpha}^t & \end{aligned} \quad (34)$$

In order to use the recursive formula (34), we need $\delta_{J\alpha}^0$. Equations (1)₅, (5) and (19)₁ give

$$\theta_0(x_1, x_2, x_3) = \sum_{\alpha=0}^K L_\alpha(x_3) \sum_{J=1}^N \phi_J(x_1, x_2) \delta_{J\alpha}(0). \quad (35)$$

Thus

$$\sum_{J=1}^N \phi_J(x_1, x_2) \delta_{J\alpha}^0 = \int_{-h/2}^{h/2} \theta_0(x_1, x_2, x_3) L_\alpha(x_3) dx_3 \equiv \hat{\theta}_0(x_1, x_2), \quad (36)$$

and

$$\left(\int_{S_I} \phi_I \phi_J dA \right) \delta_{J\alpha}^0 = \int_{S_I} \phi_I \hat{\theta}_0(x_1, x_2) dA, \quad (37)$$

which can be solved for $\delta_{J\alpha}^0$ after they have been written for all of the subdomains S_1, S_2, \dots, S_N . Values of $\delta_{J\alpha}^0$ are computed from Eq. (20) written at time $t = 0$.

We note that the Crank-Nicolson method is unconditionally stable; thus the time step is determined by the accuracy desired in the computed solution.

3.5. Imposition of essential boundary conditions

Whereas the penalty method of satisfying essential boundary conditions works well for static problems, for dynamic transient problems it may significantly reduce the time step size. Also a very large value of the penalty parameter can result in ill-conditioning of the stiffness matrices \mathbf{K}^θ , \mathbf{K}^q and/or \mathbf{H} . Here we use the matrix transformation technique to satisfy essential (or Dirichlet) boundary conditions. Let D and I denote, respectively, the set of nodes where temperature is and is not prescribed. Temporarily, we suppress the depen-

dence of temperature upon time. Writing the fictitious nodal temperatures as $\{\tilde{\delta}\}$, we rewrite Eq. (34) as

$$\tilde{\mathbf{H}}\tilde{\delta} = \tilde{\mathbf{F}}, \quad (38)$$

and

$$\{\theta\} = \begin{Bmatrix} \theta_D \\ \theta_I \end{Bmatrix} = \begin{bmatrix} \phi_{DD} & \phi_{DI} \\ \phi_{ID} & \phi_{II} \end{bmatrix} \begin{Bmatrix} \tilde{\delta}_D \\ \tilde{\delta}_I \end{Bmatrix}. \quad (39)$$

Solving the first of these equations for $\tilde{\delta}_D$, we get

$$\{\tilde{\delta}\} = \begin{Bmatrix} \tilde{\delta}_D \\ \tilde{\delta}_I \end{Bmatrix} = \begin{Bmatrix} \phi_{DD}^{-1}\theta_D \\ 0 \end{Bmatrix} + \begin{Bmatrix} -\phi_{DD}^{-1}\phi_{DI} \\ I \end{Bmatrix} \{\tilde{\delta}_I\} \quad (40)$$

where 0 and I are null and the identity matrices respectively. Substitution from (40) into (38) and the premultiplication of the resulting equation by

$$\begin{bmatrix} -\psi_{DD}\psi_{DI} \\ I \end{bmatrix}^T \text{ give} \\ \tilde{\mathbf{H}}\tilde{\delta} = \tilde{\mathbf{F}} \quad (41)$$

where

$$\begin{aligned} [\tilde{\mathbf{H}}] &= \begin{bmatrix} -\psi_{DD}^{-1}\psi_{DI} \\ I \end{bmatrix}^T [\tilde{\mathbf{H}}] \begin{bmatrix} -\phi_{DD}^{-1}\phi_{DI} \\ I \end{bmatrix} \\ [\tilde{\mathbf{F}}] &= \begin{bmatrix} -\psi_{DD}^{-1}\psi_{DI} \\ I \end{bmatrix}^T [\tilde{\mathbf{F}}] - \begin{bmatrix} -\psi_{DD}^{-1}\psi_{DI} \\ I \end{bmatrix} [\tilde{\mathbf{H}}] \begin{Bmatrix} \phi_{DD}^{-1}\theta_D \\ 0 \end{Bmatrix} \end{aligned} \quad (42)$$

4. Estimation of the effective heat capacity and thermal conductivity

We assume that inclusions are spherical and are randomly distributed in the matrix. Furthermore they are made of isotropic materials and the macroscopic response of the composite can be regarded as isotropic.

The effective heat capacity, $\rho(x_3)c(x_3)$, of the composite is computed from the rule of mixtures:

$$\rho(x_3)c(x_3) = \rho_1 c_1 V_1(x_3) + \rho_2 c_2 V_2(x_3) \quad (43)$$

where subscripts 1 and 2 denote values of a quantity for constituents 1 and 2 respectively, V_1 is the volume fraction of constituent 1, and $V_2 = 1 - V_1$. The effective thermal conductivity, κ , is computed from the following relation proposed by Hatta and Taya [9].

$$\frac{\kappa - \kappa_1}{\kappa_2 - \kappa_1} = \frac{V_2}{1 + (1 - V_2)(\kappa_2 - \kappa_1)/3\kappa_1}. \quad (44)$$

The through-the-thickness variation of V_2 is assumed to be given by

$$V_2 = V_2^- + (V_2^+ - V_2^-) \left(\frac{1}{2} + \frac{x_3}{h} \right)^p, \quad (45)$$

where superscripts + and - signify, respectively, values of the quantity on the top and the bottom surfaces of the plate, and the parameter p describes the variation of phase 2. $p = 0$ and ∞ correspond to uniform distributions of phase 2 with volume fractions V_2^+ and V_2^- respectively.

5. Computation and discussion of results

Because of the availability of analytical results [32], we analyze heat conduction in an Aluminum/Silicon Carbide (Al/SiC) rectangular plate and assign following values to various material, geometric and computational parameters.

$$L_1 = L_2 = 250\text{mm}, h = 50\text{mm},$$

$$K = 5, m = 15, b = 15, N = 13 \times 13 = 169,$$

$$N_Q = 9 \times 9 = 81,$$

$$\text{Al} : \rho_1 = 2707\text{kg/m}^3, c_1 = 896\text{J/kgK}, \kappa = 233\text{W/mK},$$

$$\text{SiC} : \rho_2 = 3100\text{kg/m}^3, c_2 = 670\text{J/kgK}, \kappa = 65\text{W/mK}. \quad (46)$$

Our previous experience [8, 23, 24, 26, 27] with the analysis of thick plates has revealed that a 5th order plate theory is adequate. Furthermore, the analysis of deformations of thick plates by the MLPG method has suggested that the use of fourth degree complete monomials in (25) to generate the MLS basis functions, 13 equally spaced nodes in the x_1 - and the x_2 -directions as shown in Fig. 2, and the 9×9 Gauss quadrature rule should give very good results. Thus for the case of the heat flux prescribed on all bounding surfaces, there are $6 \times 169 = 1014$ unknowns.

Since the heat flux or the temperature prescribed on the top ($x_3 = h/2$) or the bottom ($x_3 = -h/2$) surface can be expanded in terms of Fourier series in x_1 and x_2 , it suffices to consider the prescribed heat flux or the prescribed temperature that varies sinusoidally in the x_1 - and the x_2 -directions. Results have been computed for the following two sets of boundary conditions.

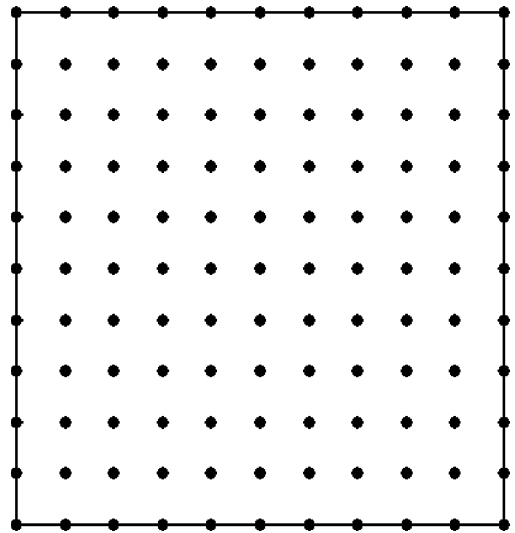


Fig. 2 Thirteen uniformly spaced nodes in the x_1 - and the x_2 -directions

(a) Heat flux prescribed on the top and the bottom surfaces.

$$\begin{aligned}
 q^+ \left(x_1, x_2, \frac{h}{2}, t \right) &= q_0^+ (1 - e^{-\gamma t}) \sin \frac{\pi x_1}{L_1} \sin \frac{\pi x_2}{L_2}, \\
 q^- \left(x_1, x_2, -\frac{h}{2}, t \right) &= 0, \\
 \theta(0, x_2, x_3, t) &= \theta(L_1, x_2, x_3, t) = 0, \\
 \theta(x_1, 0, x_3, t) &= \theta(x_1, L_2, x_3, t) = 0.
 \end{aligned}
 \tag{47}$$

The heat flux prescribed at a point on the top surface of the plate reaches its equilibrium value asymptotically. The bottom surface of the plate is thermally insulated.

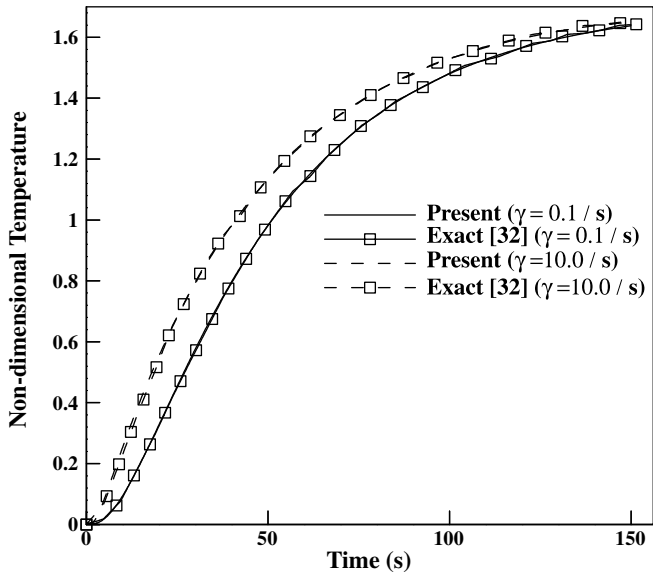
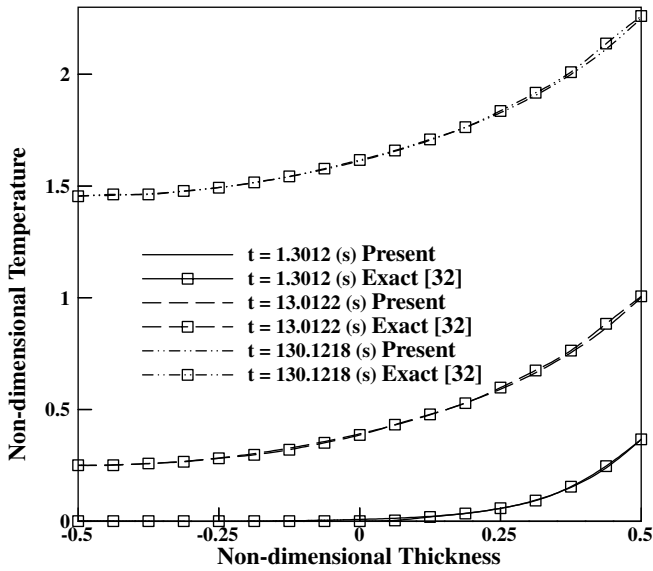


Fig. 3a, b Comparison of the computed solution with the analytical solution [32] for the case of the heat flux prescribed on the top surface; **a** through-the-thickness variation of the temperature at times $t = 1.3012, 13.0122$ and $130.1218s$, **b** time history of the temperature at the plate centroid for $\gamma = 0.1$ and $10.0/s$

Results in figs. are presented in terms of following variables.

$$\hat{\theta} = \frac{\theta \kappa_1}{q_0^+ h}, \hat{q} = q/q_0^+.
 \tag{48}$$

(b) Temperature prescribed on all bounding surfaces

$$\begin{aligned}
 \theta^+ \left(x_1, x_2, \frac{h}{2}, t \right) &= \theta_0^+ (1 - e^{-\gamma t}) \sin \frac{\pi x_1}{L_1} \sin \frac{\pi x_2}{L_2}, \\
 \theta^- \left(x_1, x_2, -\frac{h}{2}, t \right) &= 0, \\
 \theta(0, x_2, x_3, t) &= \theta(L_1, x_2, x_3, t) = 0, \\
 \theta(x_1, 0, x_3, t) &= \theta(x_1, L_2, x_3, t) = 0.
 \end{aligned}
 \tag{49}$$

Results are presented in terms of the following nondimensional variables.

$$\hat{\theta} = \theta/\theta_0^+, \hat{q} = -\frac{qh}{\kappa_1 \theta_0^+}.
 \tag{50}$$

Unless otherwise specified, results presented below are for $V_2^- = 0, V_2^+ = 1.0, p = 2.0$ and $\gamma = 10.0/s$ with Silicon Carbide as phase 2.

For the heat flux prescribed on the major surfaces of the plate, Fig. 3a, b depicts the temperature distribution through the plate thickness at $t = 1.3012, 13.0122$ and $131.1218s$, and the time histories of the temperature at the plate centroid for $\gamma = 0.1$ and $10.0/s$. It is clear that the presently computed solution matches very well with the analytical solution. Thus the order of the plate theory and values assigned to other variables are adequate to accurately compute the temperature at any point in the plate. As expected, the temperature at the plate centroid rises slowly for $\gamma = 10/s$ as compared to that for $\gamma = 0.1/s$. At $150s$, the temperature at the plate centroid is nearly the same for the two values of γ since a steady state has reached. For $V_2^- = 0.2, p = 4.0$ and $\gamma = 1/s$, Fig. 4a exhibits the influence of V_2^+ on the time history of the temperature at the plate centroid. The effect of increasing V_2^+ , i.e., the volume fraction of SiC on the top surface of the plate exposed to the heat flux, is to decrease the temperature at the plate centroid. This is because the thermal conductivity of SiC is about one-fourth that of Al and the heat capacity of SiC is nearly 0.87 times that of Al. For $\gamma = 1.0/s, V_2^+ = 0.8, V_2^- = 0.2$, and $p = 2, 4$ and 10 , Fig. 4b evinces the evolution of the temperature at the plate centroid. Note that a higher value of p implies a lower value of V_2 at a point which in turn slows down the heat conduction process. Thus the temperature at the plate centroid is higher for the lower value of p . For $V_2^+ = 0.8, V_2^- = 0.2$ and $p = 4$, Fig. 4c shows the influence of γ on the time history of the temperature rise at the plate centroid. The time histories of the temperature rise for $\gamma = 1.0$ and $10.0/s$ are virtually indistinguishable. The temperature rise is lower for $\gamma = 0.1/s$ than that for $\gamma = 1.0/s$ because the heat flux increases slowly for $\gamma = 0.1/s$. We have plotted in Fig. 5a, b through-the-thickness variations of the steady state temperature for five values of V_2^+ and four values

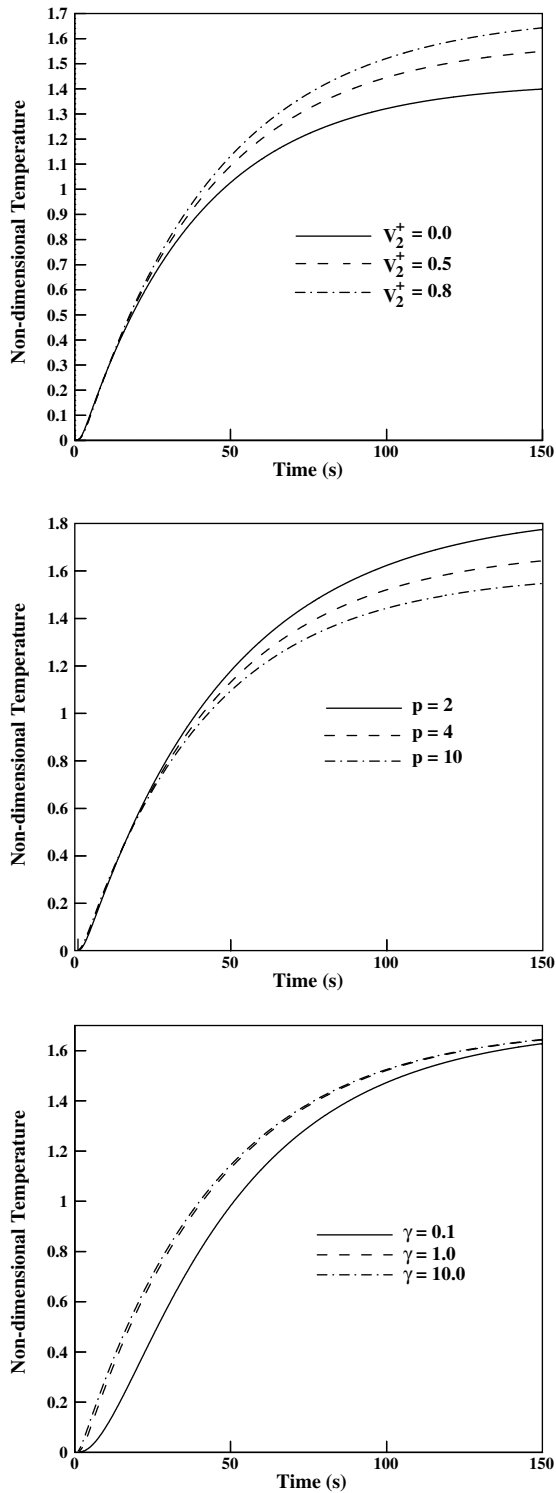


Fig. 4a For heat flux prescribed on the top surface, time histories of the temperature at the plate centroid for three values of **a** the volume fraction of SiC on the top surface, **b** the exponent p in Eq. (45), and **c** the time rise constant γ in Eq. (47)₁

of p . The temperature gradient at points near the top surface of the plate increases with an increase in the value of V_2^+ , but that near the bottom surface of the plate is essentially unaffected by the value of V_2^+ .

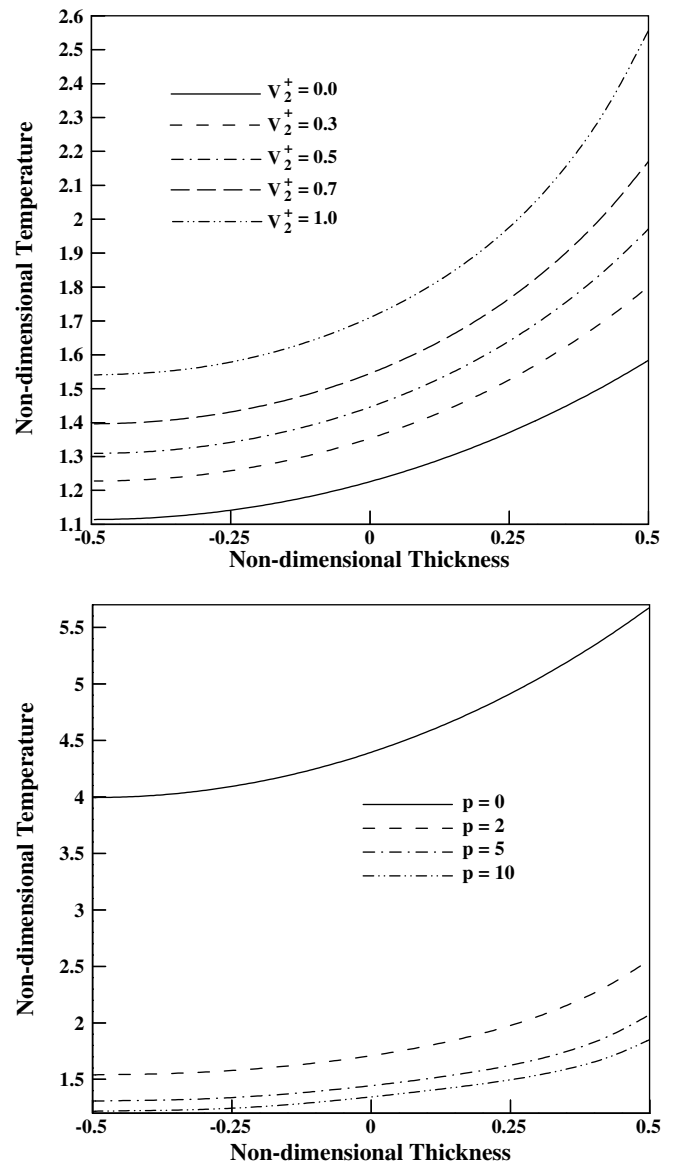


Fig. 5a Through-the-thickness variation of the temperature for heat flux prescribed on the top surface and for several values of **a** the volume fraction of SiC on the top surface, and **b** the exponent p in eq. (45)

For time-dependent temperature field prescribed on the top surface of the FG plate, Fig. 6 compares the presently computed through-the-thickness temperature distribution with the analytical solution [32]. It is clear that for each one of the three values of the time, the two solutions overlap thereby establishing the validity of the present approach. For $V_2^- = 0.2, p = 2.0, \gamma = 1.0/s$ and $V_2^+ = 0, 0.5$ and 0.8 , Fig. 7a exhibits the evolution of the temperature at the plate centroid. The time elapsed for the temperature at the plate centroid to reach a steady state value is essentially independent of the value assigned to V_2^+ , even though the rate of increase of temperature decreases with an increase in V_2^+ . The effect of increasing p with $\gamma = 1.0/s, V_2^+ = 0.8$ and $V_2^- = 0.2$ kept fixed is opposite of that of increasing V_2^+ with p held

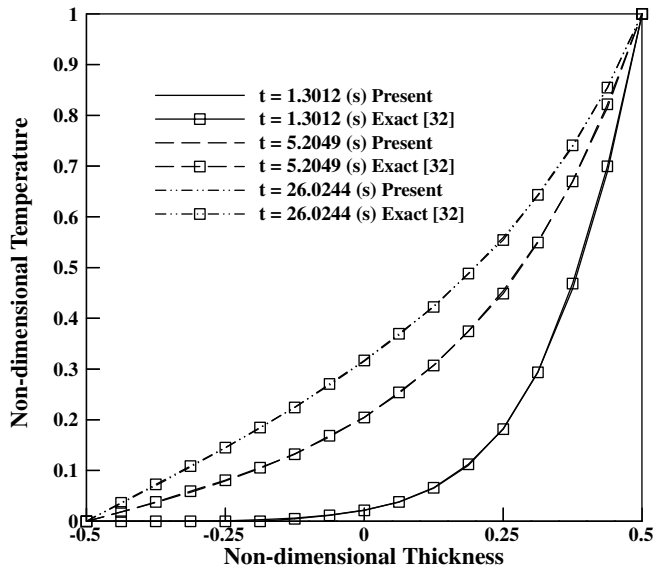


Fig. 6 Comparison of the computed solution with the analytical solution of [32] when the temperature is prescribed on the top surface; through-the-thickness variation of the temperature at times $t = 1.3012, 5.2049$ and $26.0244s$

constant. The steady state value of the temperature at the plate centroid is lower for a smaller value of p or a larger values of V_2^+ . As depicted in Fig. 7c, the temperature at the plate centroid rises very slowly for $\gamma = 0.1/s$ but the rates of increase of temperature for $\gamma = 1.0$ and $10.0/s$ are essentially the same. Note that for $\gamma = 0.1/s$, the temperature at the plate centroid has not reached the steady state value at $t = 40s$ because the prescribed temperature on the top surface of the plate is still increasing. For $\gamma = 1.0$ and $10.0/s$, the centroidal temperature becomes steady at $t \approx 15/s$. Results plotted in Fig. 7c are for $p = 4.0, V_2^- = 0.2$ and $V_2^+ = 0.8$. The steady state through-the-thickness variation of the temperature is plotted in Fig. 8a, b for five values of V_2^+ and four values of p . The temperature gradient at the bottom surface of the plate decreases with an increase in V_2^+ and that at the top surface increases. Note that the temperature distribution is not linear in a homogeneous plate because heat is conducted in x_1 - and x_2 - directions as the prescribed temperature on the top surface has a sinusoidal variation in the x_1 - and x_2 -directions. The effect of increasing p is to increase the temperature gradient near the top surface and decrease near the bottom surface. For $p = 2, 4$ and 10 , the temperature gradient at points adjacent to top surface is virtually the same but that at points near the bottom surface decreases with an increase in the value of p .

6. Conclusions

It is shown that the transient temperature distribution in a thick functionally graded plate computed by using a fifth-order plate theory and the meshless local Petrov-

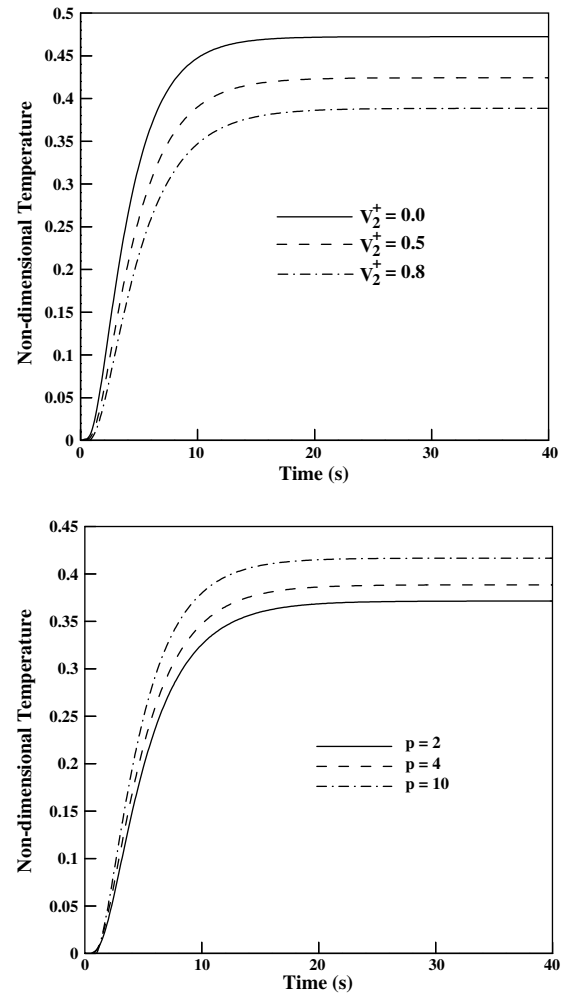


Fig. 7a For the case of the temperature prescribed on the top surface, time histories of the temperature at the plate centroid for three values of **a** the volume fraction of SiC on the top surface, **b** the exponent p in Eq. (45), and **c** the time rise constant γ in Eq. (49)₁

Galerkin method matches very well with that obtained analytically. The presumed temperature distribution through the plate thickness exactly satisfies prescribed temperature on the major surfaces of the plate.

Acknowledgements This work was partially supported by the ONR grant N0014-98-1-0300 to Virginia Polytechnic Institute and State University with Dr. Y. D. S. Rajapakse as the cognizant Program Manager. L. F. Qian was also supported by the China Scholarship Council.

References

1. Atluri SN, Zhu T (1998) A new meshless local Petrov-Galerkin (MLPG) approach in computational mechanics. *Computat. Mech.* 22: 117–127
2. Atluri SN, Shen SP (2002) *The Meshless Local Petrov-Galerkin (MLPG) Method*. Tech Science Press, California
3. Babuska I, Lee I, Schwab C (1994) On the a-posteriori estimation of the modeling error for the heat-conduction in a plate and its use for adaptive hierarchical modeling. *Appl. Numer. Math.* 14: 5–21

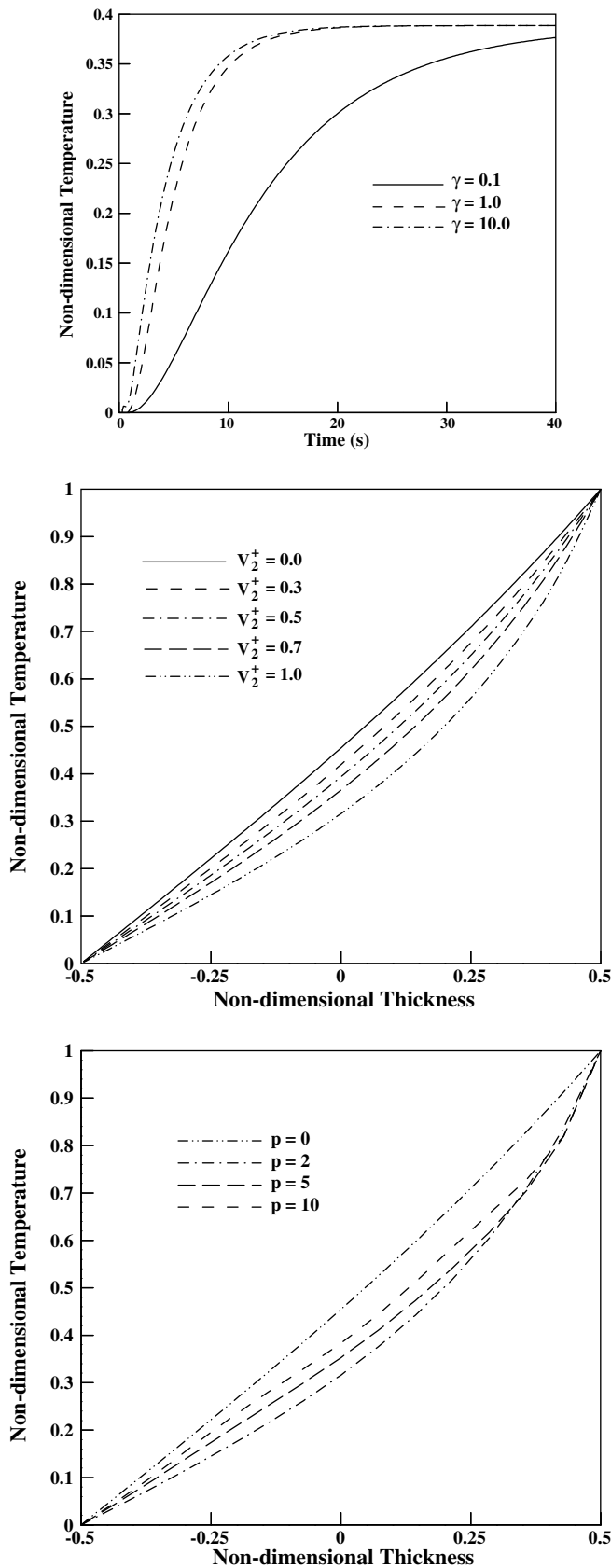


Fig. 8 Through-the-thickness variation of the temperature for the case of temperature prescribed on the top surface and for **a** values of the volume fraction of SiC on the top surface, and **b** four values of the exponent p in eqn. (45)

4. Batra RC (1980) Finite plane strain deformations of rubberlike materials. *Int. J. Numer. Meth. Eng.* 15: 145–160.
5. Batra RC, Love BM (2005) Adiabatic shear bands in functionally graded materials, *J. Thermal Stresses* (in press)
6. Batra RC, Porfiri M, Spinello D (2004) Treatment of material discontinuity in two meshless local Petrov-Galerkin (MLPG) formulations of axisymmetric transient heat conduction. *Int. J. Numer. Meth. Eng.* (accepted).
7. Batra RC, Vidoli S (2002) Higher order piezoelectric plate theory derived from a three-dimensional variational principle. *AIAA J.* 40(1): 91–104
8. Batra RC, Vidoli S, Vestroni F (2002) Plane waves and modal analysis in higher-order shear and normal deformable plate theories. *J. Sound Vibration* 257(1): 63–88
9. Belytschko T, Lu YY, Gu L (1994) Element-free Galerkin methods. *Int. J. Numer. Meth. Eng.* 37: 229–256
10. Cheng ZQ, Batra RC (2000) Three-dimensional asymptotic scheme for piezothermoelastic laminates. *J. Thermal Stresses* 23: 95–110
11. Durate CA, Oden JT (2000) H-p clouds - an hp meshless method. *Numer. Meth. Partial Differential Equations* 1–34
12. Gingold RA, Monaghan IJ (1977) Smooth particle hydrodynamics: theory and applications to non-spherical stars. *Mon. Not R. Astro. Soc.* 181: 275–389
13. Hatta H, Taya M (1985) Effective thermal conductivity of a misoriented short fiber composite. *J. Appl. Phys.* 58: 2478–2486
14. Jin Z-H, Batra RC (1996) Stress intensity relaxation at the tip of an edge crack in a functionally graded material subjected to a thermal shock. *J. Thermal Stresses* 19: 317–339
15. Kim K-S, Noda N (2001) Green's function approach to three-dimensional heat conduction equations of functionally graded materials. *J. Thermal Stresses* 24: 457–477
16. Lancaster P, Salkauskas K (1981) Surfaces generated by moving least squares method. *Comput. Mech.* 37: 141–158
17. Liu GR (2003) *Mesh Free Methods*. CRC Press, Boca Raton
18. Liu WK, Jun S, Zhang YF (1995) Reproducing kernel particle methods. *Int. J. Numer. Meth. Eng.* 20: 1081–1106
19. Lucy L (1977) A numerical approach to testing the fission hypothesis. *Astronomical J.* 82: 1013–1024
20. Melenk JM, Babuska I (1996) The partition of unity finite element method: Basic theory and applications. *Comput. Meth. Appl. Mech. Eng.* 139: 289–314
21. Nayroles B, Touzot G, Villon P (1992) Generalizing the finite element method: Diffuse approximation and diffuse elements. *Comput. Mech.* 10: 307–318
22. Ootao Y, Tanigawa Y (1999) Three-dimensional transient thermal stresses of functionally graded rectangular plate due to partial heating. *J. Thermal Stresses* 22: 35–45
23. Qian LF, Batra RC, Chen LM (2003) Elastostatic deformations of a thick plate by using a higher-order shear and normal deformable plate theory and two meshless local Petrov-Galerkin (MLPG) methods. *Comput. Model. Eng. and Sci.* 4: 161–176
24. Qian LF, Batra RC, Chen LM (2003) Free and forced vibrations of thick rectangular plates by using higher-order shear and normal deformable plate theory and meshless local Petrov-Galerkin (MLPG) method. *Comput. Model. Eng. and Sci.* 4: 519–534
25. Qian LF, Batra RC, Chen LM (2004) Analysis of cylindrical bending thermoelastic deformations of functionally graded plates by a meshless local Petrov-Galerkin method. *Comput. Mech.* 33: 263–273
26. Qian LF, Batra RC (2004) Transient thermoelastic deformations of a thick functionally graded plate. *J. of Thermal Stresses.* 27: 705–740
27. Qian LF, Batra RC, Chen LM (2004) Static and dynamic deformations of thick functionally graded elastic plate by using higher-order shear and normal deformable plate theory and meshless local Petrov-Galerkin method. *Composites: Part B.* 35: 685–697

28. Rössle A, Bischoff M, Wendland W, Ramm E (1999) On the mathematical foundation of the (1,1,2)-plate model. *Int. J. Solids Structures*. 36: 2143–2168
29. Sladek J, Sladek V, Zhang C (2003) Transient heat conduction analysis in functionally graded materials by the meshless local boundary integral equation method. *Comput. Mat. Sci.* 28: 494–504
30. Sukumar N, Moran B, Belytschko T (1998) The natural element method in solid mechanics. *Int. J. Numer. Meth. Eng.* 43: 839–887
31. Sutradhar A, Paulino GH, Gray LJ (2002) Three-dimensional transient heat conduction in functionally graded materials. *Proc. Int. Assoc. Boundary Element Methods*, Univ. of Texas, Austin
32. Vel SS, Batra RC (2003) Three-dimensional analysis of transient thermal stresses in functionally graded plates. *Int. J. Solids Structures* 40: 7181–7196
33. Vel SS, Batra RC (2002) Exact solutions for thermoelastic deformations of functionally graded thick rectangular plates. *AIAA J.* 40(7): 1255–1273
34. Vel SS, Batra RC (2003) Generalized plane strain thermopiezoelectric analysis of multilayered plates. *J. Thermal Stresses*. 26: 353–377
35. Vel SS, Batra RC (2001) Generalized plane strain thermoelastic deformation of laminated anisotropic thick plates. *Int. J. Solids Structures*. 38: 1395–1414
36. Warlock A, Ching H-K, Kapila AK, Batra RC (2002) Plane strain deformations of an elastic material compressed in a rough rectangular cavity. *Int. J. Eng. Sci.* 40: 991–1010
37. Wendland H (1995) Piecewise polynomial, positive definite and compactly supported radial basis functions of minimal degree. *Adv. Comput. Meth.* 4: 389–396
38. Zhang GM, Batra RC (2004) Modified smoothed particle hydrodynamics method and its application to transient problems. *Comput. Mech.* 34: 137–146